



Research article

Optimization of an integrated feedback control for a pest management predator-prey model

Zhenzhen Shi¹, Huidong Cheng^{1,*}, Yu Liu² and Yanhui Wang¹

¹ College of Mathematics and System Sciences, Shandong University of Science and Technology, Qingdao 266590, Shandong, China

² College of Foreign Languages, Shandong University of Science and Technology, Qingdao 266590, Shandong, China

* **Correspondence:** Emil: chd900517@sdust.edu.cn; Tel: +053288032097.

Abstract: In this paper, a Leslie-Gower predator-prey model with ratio-dependence and state pulse feedback control is established to investigate the effect of spraying chemical pesticides and supplement amount of beneficial insects at the same time. Firstly, the existence, uniqueness and asymptotic stability of the periodic solution are proved by using successor function method and the analogue of the Poincaré criterion when the equilibria E_* and E_0 are stable, and the existence of limit cycles without impulse system is verified when the equilibrium E_* is unstable. Furthermore, to obtain the minimum cost per period of controlling pests, we propose the optimization problem and calculate the optimal threshold. Finally, the feasibility of our model is proved by numerical simulation of a concrete example.

Keywords: semi-continuous dynamic systems; order-1 periodic solution; successor functions; limit cycle; optimization

1. Introduction

In the real world, the threat of pests to agriculture is growing. How to control the pest quantity effectively in agricultural development has become one of the important problems. In the past decades, many researchers have paid their attention in finding methods to control pest populations, and there are some good results [1–8].

There are three main methods of controlling pests. One is the use of chemical control methods, namely spraying insecticide. Its disadvantage is that it pollutes the environment or products and also causes the ecological imbalance because of the massive death of predators evenly. The second is the use of biological control which can make full use of the role of natural control in the agricultural ecosystem, that is, to reduce the population density of pests effectively by artificially raising natural enemies and

releasing them periodically. However this method is only applicable to the smaller density of the pest population and once the pest population exceeds a certain number, the method will be invalid. The third method is the integrated control method of chemical control and biological control, which is the most widely used method in the agricultural and ecological resource management. If the density of the pest population is lower than the economic threshold, then it is not necessary to adopt any control strategy, but once the pest population density reaches or exceeds the economic threshold, we should adopt a certain control strategy to avoid the imbalance of ecology. In this paper, we apply state dependent impulsive differential equations to describe the implementation of the feedback control strategy.

In recent years, semi-continuous dynamical system theory has been applied in many fields such as biology, ecology and economics [9–17]. In [18, 19], the integrated control system with state pulse feedback control was considered, some sufficient conditions of the existence and uniqueness of the periodic solution were obtained by the successor function method, and the stability of the periodic solution was proved. In [20], the related properties of the Leslie-Gower model without impulse were studied. In [21, 22], the dynamic properties of periodic solutions of the predator-prey model were investigated. In [23], Pei *et al.* applied the time pulse method to harvest the prey at fixed time. Jiao *et al.* [24] mainly considered the periodic pulsed predator-prey model during hibernation and obtained the global asymptotic stability criterion for the extinction boundary of the predators.

Although there are fruitful results on mathematical models with state dependence on the pulse feedback control, but most of them are just based on the study of a single pulse control and few of them considered the feedback control strategy for two different influence of the prey and predators at the same time. These researches were rare on that how to control pesticide spraying to get greater economic benefits [25–27]. Therefore, we construct a Leslie-Gower model with ratio-dependence and state pulse feedback control in this paper.

The structure of this paper is as follows: In Section 2, we build a Leslie-Gower predator-prey model with ratio-dependence and state pulse control. This is a generalisation of the original Leslie model with ratio-dependence by adding the state pulse feedback control. In Section 3, the existence, uniqueness and the asymptotic stability of the periodic solution are proved according to the relevant characteristics of the positive equilibrium point E_* . In Section 4, we formulate an optimal problem and obtain the economic threshold. In addition, some numerical simulation examples are carried out to verify our theoretical results. We give a short conclusion in Section 5.

2. Model building

The Leslie model is one of the most classic prey-predator model, and have modified and improved many scholars to modify and improve it in many aspects [28–31]. Especially, due to the laboratory experiments [32–36] and observation [37–43], a few of researchers focus on the ratio-dependence of the Leslie prey-predator model recently. Gupta et al constructed Leslie-Gower predator-prey model with Michaelis-Menten type prey-harvesting and investigated bifurcations of the model [44]. In [45], Zhao et al established a Leslie-Gower predator-prey system with fixed time impulsive and discussed the persistence of system. However, state dependent pulse differential system is more in line with the actual biological the system. Wei et al [46] proposed a Leslie-Gower pest management model with impulsive state feedback control and discussed the conditions for existence and stability of periodic solutions. Flores and E. González-Olivares proposed a modified Leslie-Gower predator-prey model

with ratio-dependent functional response and alternative food for the predator [47].

In [48], Liang et al. established the following Leslie-Gower model with ratio-dependence:

$$\begin{cases} x_1'(t_1) = rx_1(t_1) \left(1 - \frac{x_1(t_1)}{K}\right) - \frac{kx_1(t_1)y_1(t_1)}{a_1y_1(t_1) + x_1(t_1)}, \\ y_1'(t_1) = y_1(t_1)a_2 \left(1 - c\frac{y_1(t_1)}{x_1(t_1)}\right). \end{cases} \quad (2.1)$$

In System (2.1), $x_1(t_1)$, $y_1(t_1)$ represent the densities of prey(pest) and predators (natural enemies) at time t_1 , respectively. a_2 is the intrinsic rate of growth of natural enemies. Environmental carrying capacity is proportional to the maximum amount of food that the environment can hold, that means, $K(x) = x/b$. The natural enemies' consumption of the pest depends on the ratio $\frac{kx_1}{a_1y_1+x_1}$, where k is the maximum amount of the pest. The parameter c represents the maximum value of the average deficit reduction of y_1 to x_1 , $c\frac{y_1}{x_1}$ is named the Leslie-Gower pattern. In addition, the parameters r , a_1 , a_2 , k , c , K are all positive constants.

According to the Introduction, ET_1 denotes the pest slightly harmful threshold. When the number of the pest population achieves ET_1 , we only need to adopt biological control strategies to reduce effectively the number of pests. Analogously, ET_2 denotes the pest economic injury threshold. When the number of pests achieves ET_2 , only by adopting chemical control strategy can the pest quantity be reduced effectively in a short time. However, in most cases, the control strategy we adopt is the integrated control strategy. In this paper, we apply the integrated control strategy to achieve effective control of pests when the number of pests satisfies $x_1 \in [ET_1, ET_2]$. To achieve this objective, we establish a model as follows:

$$\begin{cases} \left. \begin{aligned} x_1'(t_1) &= rx_1(t_1) - \frac{r(x_1(t_1))^2}{K} - \frac{kx_1(t_1)y_1(t_1)}{a_1y_1(t_1) + x_1(t_1)}, \\ y_1'(t_1) &= a_2y_1(t_1) - ca_1\frac{y_1(t_1)}{x_1(t_1)}y_1(t_1), \end{aligned} \right\} x_1(t_1) < ET \\ \left. \begin{aligned} \Delta x_1(t_1) &= -p(x_1)x_1(t_1), \\ \Delta y_1(t_1) &= -q(x_1)y_1(t_1) + \tau(x_1), \end{aligned} \right\} x_1(t_1) = ET, \end{cases} \quad (2.2)$$

where $ET \in [ET_1, ET_2]$. When the number of pests is less than the economic threshold ET , we adopt biological control strategy for pests. When the number of pests is greater than the economic threshold ET , the pests are adopted integrated control strategy. Consider the dynamic behavior of System (2.2), the proportionality coefficient of the amount of the killed pests and natural enemies are defined as $p(x_1)(p(x_1) \in (0, 1))$ and $q(x_1)(0 < q(x_1) < p(x_1))$, and $\tau(x_1)$ is defined as the number of artificial natural enemies. To simplify, we nondimensionalize System (2.2) by using $rt_1 = t$, $\frac{x_1(t_1)}{K} = x(t)$, and $\frac{ky_1(t_1)}{r} = y(t)$. Then we get the following form:

$$\begin{cases} \left. \begin{aligned} x'(t) &= x(t) - x^2(t) - \frac{x(t)y(t)}{\alpha_1y(t) + x(t)}, \\ y'(t) &= \alpha_2\beta y(t) - \frac{\beta y^2(t)}{x(t)}, \end{aligned} \right\} x(t) < \xi, \\ \left. \begin{aligned} \Delta x(t) &= -p(x)x(t), \\ \Delta y(t) &= -q(x)y(t) + \tau(x), \end{aligned} \right\} x(t) = \xi, \end{cases} \quad (2.3)$$

where $\alpha_1 = \frac{a_1 r}{kK}$, $\alpha_2 = \frac{a_2 kK}{rca_1}$, $\beta = \frac{a_1 c}{kK}$, and $\xi = \frac{ET}{K}$.

$$\begin{cases} p(x) = p_{max} \frac{x - \xi_{min}}{\xi_{max} - \xi_{min}}, \\ \tau(x) = \tau_{max} - (\tau_{max} - \tau_{min}) \frac{x - \xi_{min}}{\xi_{max} - \xi_{min}}, \\ q(x) = q_{max} \frac{x - \xi_{min}}{\xi_{max} - \xi_{min}}. \end{cases} \quad (2.4)$$

The control parameters $p(x)$, $q(x)$, $\tau(x)$ are continuous functions defined on $[\xi_{min}, \xi_{max}]$, ξ_{min} and ξ_{max} are the minimum value and maximum value respectively, which satisfy $0 < \xi_{max} \leq \xi \leq \xi_{max} < \frac{K}{1-p_{min}}$. In addition, $p(\xi_{max}) = p_{max}$, $\tau(\xi_{max}) = \tau_{min}$, $\tau(\xi_{min}) = \tau_{max}$ and $q(\xi_{max}) = q_{max}$. Denote $p_\xi = p(\xi)$, $\tau_\xi = \tau(\xi)$ and $q_\xi = q(\xi)$, we may see [49] for more details.

In the absence of impulses, the predator-prey model is as follows:

$$\begin{cases} x'(t) = x(t) - x^2(t) - \frac{x(t)y(t)}{\alpha_1 y(t) + x(t)}, \\ y'(t) = \alpha_2 \beta y(t) - \frac{\beta y^2(t)}{x(t)}. \end{cases} \quad (2.5)$$

The isoclinic line $L_1 : 1 - x - \frac{1}{\alpha_1 y + x} y = 0$ has the following features: when the value range of x is $(0, 1)$, first, if the condition $\alpha_1 = 1$ holds, then the line L_1 denotes a straight line; second, if the condition $\alpha_1 < 1$ holds, then the line L_1 signifies an opening downward curve line; third, if the condition $\alpha_1 > 1$ holds, then the line L_1 signifies an opening upward curve line. According to the practical significance, we only discuss the condition $\alpha_1 < 1$ in our research. It can be known from [48] that if $\alpha_1 \alpha_2 + 1 > \alpha_2$ holds, then System (2.5) exists a positive equilibrium $E_*(x_*, y_*)$, where $x_* = 1 - \frac{\alpha_2}{\alpha_1 \alpha_2 + 1}$, $y_* = \alpha_2 x_*$. The equilibrium $E_0(1, 0)$ is a saddle point that the stable manifold is located on the positive x axis.

Lemma 1 [48] If condition $\alpha_1 > 1$ holds, then system (5) is permanent.

Lemma 2 [48] The equilibrium $E_0(1, 0)$ of system (5) is a saddle point with the positive x -axis as its stable manifold.

Lemma 3 [48] If conditions $\alpha_1 \cdot \alpha_2 + 1 > \alpha_2$ and $(\alpha_1 \alpha_2 + 2)\alpha_2 < (\beta \alpha_2 + 1)(\alpha_1 \cdot \alpha_2 + 1)^2$ hold, then the positive equilibrium $E_*(x_*, y_*)$ of system (2.5) is a locally asymptotically stable node or focus. If conditions $\alpha_1 \alpha_2 + 1 > \alpha_2$ and $(\alpha_1 \alpha_2 + 2)\alpha_2 > (\beta \alpha_2 + 1)(\alpha_1 \cdot \alpha_2 + 1)^2$ hold, then the positive equilibrium $E_*(x_*, y_*)$ of system (2.5) is an unstable node or focus. In addition, system (2.5) has a unique limit cycle. The vector field of System (2.5) is shown in Figure 1.

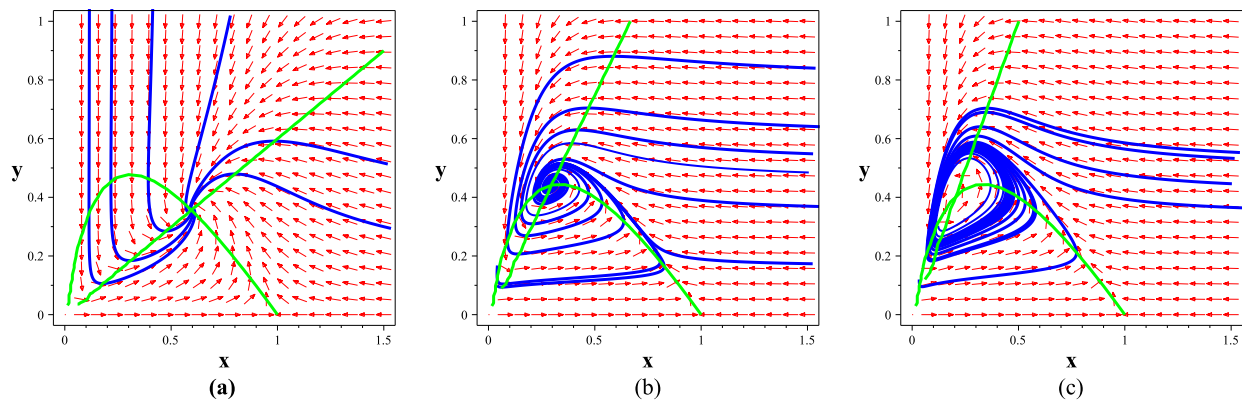


Figure 1. The phase diagram of System (2.5). (a) Parameters value: $\alpha_1 = 0.8$, $\alpha_2 = 0.6$, $\beta = 1.5$. E_* is a stable node. (b) Parameters value: $\alpha_1 = 0.75$, $\alpha_2 = 1.5$, $\beta = 0.05$. E_* is a stable focus. (c) Parameters value: $\alpha_1 = 0.75$, $\alpha_2 = 2$, $\beta = 0.05$. Limit cycle.

By [50, Definition 2.1], system (2.3) is a semi-continuous power system. For system (2.3), the impulse set is $\sum_M = \{(x, y) \in \mathbb{R}_+^2 | x = \xi, y \geq 0\}$, the pulse mapping is $\varphi : (x, y) \in \sum_M \rightarrow ((1 - p(\xi))x, (1 - q(\xi))y + \tau) \in \mathbb{R}_+^2$, and the image set is $\sum_N = \varphi(\sum_M) = \{(x, y) \in \mathbb{R}_+^2 | x = (1 - p_\xi)\xi, y \geq 0\}$.

For any point T , x_T and y_T are denoted its horizontal coordinate and vertical coordinate, respectively. If $T \in \sum_M$, then the impulse starts at the point T , and the impulse function will run from T to \sum_N . Considering the ecological practice, we apply system (2.3) to the space \mathbb{R}_+^2 .

3. Dynamical analysis of system (2.3)

In two aspects, we prove the existence, uniqueness and asymptotic stability of periodic solutions: $\xi \leq \min\{x_*, \xi_{max}\}$ and $\max\{x_*, \xi_{min}\} < \xi < 1$.

3.1. When $\xi \leq \min\{x_*, \xi_{max}\}$

Theorem 3.1. *If conditions $\alpha_1 \cdot \alpha_2 + 1 > \alpha_2$, $\xi \leq \min\{x_*, \xi_{max}\}$ and $(\alpha_1 \alpha_2 + 2)\alpha_2 < (\beta \alpha_2 + 1)(\alpha_1 \alpha_2 + 1)^2$ hold, then system (2.3) possesses order-1 periodic solution.*

Proof. According to Theorem 1, we can see that the positive equilibrium $E_*(x_*, y_*)$ is stable.

The isoclinic line $L_1 : 1 - x - \frac{y}{\alpha_1 y + x} = 0$ intersects with the image set \sum_N at the point A . The trajectory with the initial point A intersects with the impulse set \sum_M at point A_1 , then runs to the point $A_1^+ \in \sum_N$ with impulse effects. According to the location of point A_1^+ , there may be three possible scenarios : (1) $y_{A_1^+} = y_A$, (2) $y_{A_1^+} > y_A$, (3) $y_{A_1^+} < y_A$.

Now, we prove each of these cases separately.

Case I: $y_{A_1^+} = y_A$.

In this case, A_1^+ coincides with A , and the successor function of A is $I(A) = y_{A_1^+} - y_A = 0$. According to [51, Definition 2.2], then we shall get that system (2.3) possesses order-1 periodic solutions in case of $y_{A_1^+} = y_A$ (see Figure 2(a)).

$$\begin{aligned}
& I(P) - I(Q) \\
&= (y_{P_1^+} - y_P) - (y_{Q_1^+} - y_Q) \\
&= (y_Q - y_P) + (y_{P_1^+} - y_{Q_1^+}) \\
&= (y_Q - y_P) + (1 - q)y_{P_1} + \tau - (1 - q)y_{Q_1} - \tau \\
&= (y_Q - y_P) + (1 - q)(y_{P_1} - y_{Q_1}) > 0,
\end{aligned}$$

The successor function is monotonically increasing in the $\overline{AA_1^+}$, thus there is only one point $T \in (A, A_1)$ which makes $I(T) = 0$, i.e. system (2.3) has a unique order-1 periodic solution. This proof is completed. \square

Theorem 3.3. *If conditions $\alpha_1 \cdot \alpha_2 + 1 > \alpha_2$, $(\alpha_1 \alpha_2 + 2)\alpha_2 < (\beta \alpha_2 + 1)(\alpha_1 \alpha_2 + 1)^2$ and $(1 - q) |\Theta(f_0, g_0)| < |\Theta(f_1, g_1)|$ hold, then the order-1 periodic solution of System(2.3) is orbitally asymptotically stable, where $\Theta(x, y) = \frac{1}{y}(1 - x - \frac{y}{\alpha_1 y + x})$.*

Proof. We denote that $x = f(t)$, $y = g(t)$ is a T -periodic solution of system (2.3) and $f_1 = f(T) = \xi$, $g_1 = g(T)$; $f_0 = f(0)$, $g_0 = g(0)$; $f_1^+ = f(T^+)$, $g_1^+ = g(T^+)$, then we have

$$f_1^+ = f_0 = (1 - p)\xi, \quad g_1^+ = g_0 = (1 - q)g_1 + \tau.$$

Let $P(x, y) = x - x^2 - \frac{xy}{\alpha_1 y + x}$, $Q(x, y) = \alpha_2 \beta y - \frac{\beta y^2}{x}$, $\Phi(x, y) = -p_\xi x$, $\Psi(x, y) = -q_\xi y + \tau_\xi$, $\Upsilon(x, y) = x - \xi$. Then $\frac{\partial \Phi}{\partial x} = -p$, $\frac{\partial \Psi}{\partial x} = 0$, $\frac{\partial \Phi}{\partial y} = 0$, $\frac{\partial \Psi}{\partial y} = -q$, $\frac{\partial \Upsilon}{\partial x} = 1$, $\frac{\partial \Upsilon}{\partial y} = 0$,

$$\begin{aligned}
\Delta_1 &= \frac{P_+ \left(\frac{\partial \Psi}{\partial y} \frac{\partial \Upsilon}{\partial x} - \frac{\partial \Psi}{\partial x} \frac{\partial \Upsilon}{\partial y} + \frac{\partial \Upsilon}{\partial x} \right)}{P \frac{\partial \Upsilon}{\partial x} + Q \frac{\partial \Upsilon}{\partial y}} + \frac{Q_+ \left(\frac{\partial \Phi}{\partial x} \frac{\partial \Upsilon}{\partial y} - \frac{\partial \Phi}{\partial y} \frac{\partial \Upsilon}{\partial x} + \frac{\partial \Upsilon}{\partial y} \right)}{P \frac{\partial \Upsilon}{\partial x} + Q \frac{\partial \Upsilon}{\partial y}} \\
&= \frac{P(f_1^+, g_1^+)(-q \times 1 - 0 \times 0 + 1)}{P(f_1, g_1) \times 1 + Q(f_1, g_1) \times 0} \\
&+ \frac{Q(f_1^+, g_1^+)(-p \times 0 - 0 \times 1 + 0)}{P(f_1, g_1) \times 1 + Q(f_1, g_1) \times 0} \\
&= \frac{(1 - q) \left[f_0 - f_0^2 - \frac{f_0 g_0}{\alpha_1 g_0 + f_0} \right]}{f_1 - f_1^2 - \frac{f_1 g_1}{\alpha_1 g_1 + f_1}}
\end{aligned}$$

and

$$\begin{aligned}
& \int_0^T \left(\frac{\partial P}{\partial x} + \frac{\partial Q}{\partial y} \right) dt \\
&= \int_0^T \left[1 - x - \frac{y}{\alpha_1 y + x} + \alpha_2 \beta - \frac{\beta y}{x} \right] dt \\
&+ \int_0^T \left[-x + \frac{xy}{(\alpha_1 y + x)^2} - \frac{\beta y}{x} \right] dt \\
&= \int_0^T \left[\frac{\dot{x}(t)}{x(t)} + \frac{\dot{y}(t)}{y(t)} \right] dt + \int_0^T \left[-x + \frac{xy}{(\alpha_1 y + x)^2} - \frac{\beta y}{x} \right] dt
\end{aligned}$$

$$\begin{aligned}
&= \ln \frac{x(T)y(T)}{x(0)y(0)} + \int_0^T \left[-x + \frac{xy}{(\alpha_1 y + x)^2} - \frac{\beta y}{x} \right] dt \\
&= \ln \frac{f_1 g_1}{f_0 g_0} + \int_0^T \left[-x + \frac{xy}{(\alpha_1 y + x)^2} - \frac{\beta y}{x} \right] dt
\end{aligned}$$

Furthermore,

$$\begin{aligned}
\mu_2 &= \Delta_1 \exp \int_0^T \left[\frac{\partial P}{\partial x}(f(t), g(t)) + \frac{\partial Q}{\partial y}(f(t), g(t)) \right] dt, \\
&= \frac{(1-q)f_0 \left(1 - f_0 - \frac{g_0}{\alpha_1 g_0 + f_0}\right)}{f_1 \left(1 - f_1 - \frac{g_1}{\alpha_1 g_1 + f_1}\right)} \\
&\quad \cdot \exp \left[\ln \frac{f_1 g_1}{f_0 g_0} + \int_0^T \left[-x + \frac{xy}{(\alpha_1 y + x)^2} - \frac{\beta y}{x} \right] dt \right] \\
&= \frac{(1-q)g_1 \left(1 - f_0 - \frac{g_0}{\alpha_1 g_0 + f_0}\right)}{g_0 \left(1 - f_1 - \frac{g_1}{\alpha_1 g_1 + f_1}\right)} \\
&\quad \cdot \exp \left(\int_0^T \left[-x + \frac{xy}{(\alpha_1 y + x)^2} - \frac{\beta y}{x} \right] dt \right).
\end{aligned}$$

According to biological significance, for any point (x, y) which satisfies $0 < x < \xi < 1$, $y < \frac{\xi(1-\xi)}{1-\alpha_1+\alpha_1\xi}$, then

$$-x + \frac{xy}{(\alpha_1 y + x)^2} - \frac{\beta y}{x} < 0$$

and due to $(1-q) \left| \Theta(f_0, g_0) \right| < \left| \Theta(f_1, g_1) \right|$, thus we can get

$$\left| \frac{(1-q)g_1 \left(1 - f_0 - \frac{g_0}{\alpha_1 g_0 + f_0}\right)}{g_0 \left(1 - f_1 - \frac{g_1}{\alpha_1 g_1 + f_1}\right)} \right| < 1,$$

Therefore the convergency ratio $|\mu_2|$ is less than one. Following the analogue of the Poincaré criterion [52, Theorem 2.3], we know that the order-1 periodic solution of system (2.3) is orbitally asymptotically stable. According to the above analysis, the conclusion is obtained. \square

3.2. When $\max\{x_*, \xi_{min}\} < \xi < 1$ holds.

3.2.1. The equilibrium point $E_*(x_*, y_*)$ is a stable focus.

Learning from the fourth equations of system (2.3): $\Delta y = -qy + \tau$, there exists three cases in Figure 3: (1) $\tau > \gamma$, (2) $\tau = \gamma$, (3) $\tau < \gamma$, where $\gamma = y_A - (1-q)y_{A_1}$ on the bases of value τ . Therefore, we can get following conclusions:

Theorem 3.4. In case of $\max\{x_*, \xi_{min}\} < \xi < 1$, $\alpha_1 \cdot \alpha_2 + 1 > \alpha_2$ and $(\alpha_1 \alpha_2 + 2)\alpha_2 < (\beta \alpha_2 + 1)(\alpha_1 \alpha_2 + 1)^2$, the system (2.3) has order-1 periodic solution.

Proof. We choose $\tau < \gamma$ as an example to prove (see Figure 3(b)).

In this case, $y_{A_1^+} = (1 - q)y_{A_1} + \tau < (1 - q)y_{A_1} + y_A - (1 - q)y_{A_1} = y_A$. We denote the isoclinic line $L_1 : 1 - x - \frac{y}{\alpha_1 y + x} = 0$ hitting the image set Σ_N at point A . The trajectory starting from the point A intersects the impulse set Σ_M at the point A_1 , then runs to the point A_1^+ with impulse effects. The point A_1^+ is the successor point of the point A , and A_1^+ lies under A , that is $y_{A_1^+} < y_A$, it is easy to verify that the successor function $I(A) = y_{A_1^+} - y_A < 0$. Denote the intersection point of the image set Σ_N and x axis as D . The trajectory, which starts from the initial point D , reaches the point D_1 in the impulse set Σ_M , then runs to the point D_1^+ . The point D_1^+ is the successor point of the point D , and the point D_1^+ is above the point D , that means $y_{D_1^+} > y_D$, obviously, the successor function $I(D) = y_{D_1^+} - y_D > 0$.

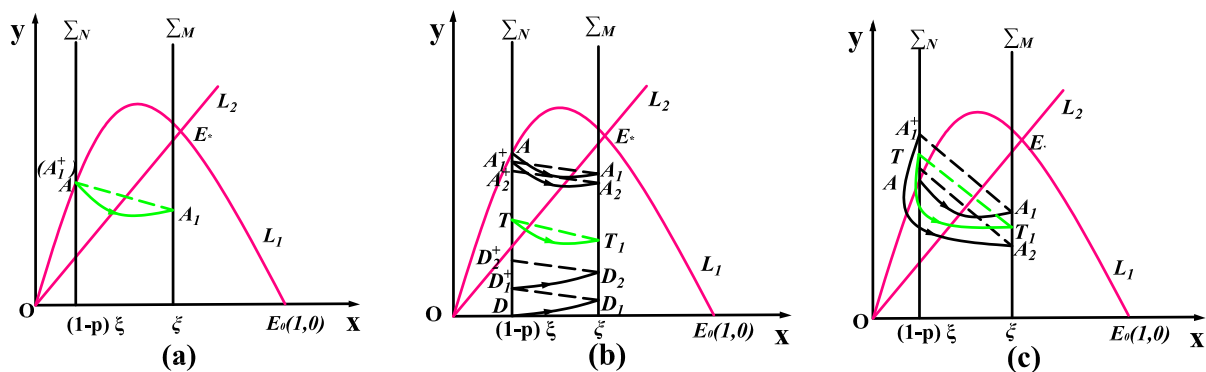


Figure 3. Three cases of successor and order-1 periodic solution. (a) $\tau = \gamma$. (b) $\tau < \gamma$. (c) $\tau > \gamma$.

Therefore, there must exist a point T , which makes $I(T) = 0$. Considering [51, Lemma 2.3], the system (2.3) has an order-1 periodic solution between the point D and the point A . This proof is done. \square

3.2.2. The equilibrium $E_*(x_*, y_*)$ is an unstable focus.

Now, let us consider the following case: if $\alpha_1\alpha_2 + 1 > \alpha_2$ and $(\alpha_1\alpha_2 + 2) > (\beta\alpha_2 + 1)(\alpha_1\alpha_2 + 1)^2$ hold, the positive equilibrium E_* of System (2.5) is an unstable node or focus, then there must exist a unique limit cycle [51, Lemma 2.2] of System (2.5). In the following sections, we will mainly discuss the case that the positive equilibrium $E_* = (x_*, y_*)$ is an unstable focus.

We denote the limit cycle as L_0 , then the limit cycle hits the isoclinic line $L_1 : 1 - x - \frac{y}{\alpha_1 y + x} = 0$ at the point $B_0(\xi_1, y_{B_0})$ and the point $B(\xi_2, y_B)$, where $\xi_1 < \xi_2$. Obviously, $\xi_1 < x_* < \xi_2$. We make two straight lines: $l_1 : x = \xi_1$, $l_2 : x = \xi_2$, and the limit cycle is sandwiched between l_1 and l_2 .

Case I: $\min\{1, \xi_{max}\} > \xi > \max\{\xi_2, \xi_{min}\}$ and $(1 - p)\xi > \xi_2$.

When $\xi > \max\{\xi_2, \xi_{min}\}$ holds, then the limit cycle lies on the left of the impulse set Σ_M , we denote function $G(M) = M^-$ as the trajectory starting from the point $M \in \Sigma_N$ and hitting the impulse set Σ_M

at the point M^- . Set $G(C) = C^-$, where C^- is the intersection of impulse set Σ_M and isoclinic line L_1 . Denote C^+ as the successor point of point C , there also exists three possible scenarios : $y_{C^+} > y_C$, $y_{C^+} = y_C$ and $y_{C^+} < y_C$ (see Figure 4).

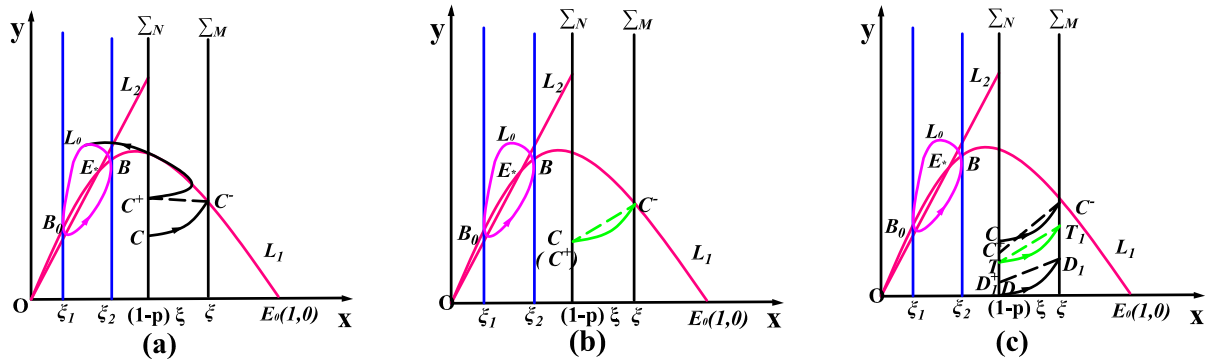


Figure 4. When $\xi > \max\{\xi_2, \xi_{min}\}$ and $(1-p)\xi > \xi_2$. (a) $y_C < y_C^+$ (b) $y_C = y_C^+$ (c) $y_C > y_C^+$.

When $y_{C^+} > y_C$, as is shown in Figure 4(a), then the motion trajectory of system (2.3) will go on for approaching the limit cycle by the several time pulse; when $y_{C^+} = y_C$ or $y_{C^+} < y_C$ hold (see Figure 4(b) and Figure 4(c), respectively), then system (2.3) has an order-1 periodic solution. Similar to the proof of Case I and Case III in Theorem 2, we can prove the existence of the order-1 periodic solution.

Therefore, we have the following conclusions:

Theorem 3.5. When $\alpha_1\alpha_2 + 1 > \alpha_2$, $(\alpha_1\alpha_2 + 2)\alpha_2 > (\beta\alpha_2 + 1)(\alpha_1\alpha_2 + 1)^2$, $\xi > \max\{\xi_2, \xi_{min}\}$ and $(1-p)\xi > \xi_2$ hold, if y_{C^+} satisfies $y_{C^+} > y_C$, then the trajectory of system (2.3) will approach to the limit cycle L_0 in the end.

Case II: $\xi > \max\{\xi_2, \xi_{min}\}$ and $\xi_1 < (1-p)\xi < \xi_2$.

Theorem 3.6. When $\alpha_1\alpha_2 + 1 > \alpha_2$, $(\alpha_1\alpha_2 + 2)\alpha_2 > (\beta\alpha_2 + 1)(\alpha_1\alpha_2 + 1)^2$, $\xi > \max\{\xi_2, \xi_{min}\}$ and $\xi_1 < (1-p)\xi < \xi_2$ hold, then the trajectory of system (2.3) will approach to the limit cycle L_0 in the end.

Proof. The trajectory starting from the point D either intersects with the impulse set Σ_M or disjoins with the impulse set Σ_M , therefore, we discuss the two cases separately in the following.

If the trajectory disjoins with the impulse set Σ_M , the trajectory must approach to the limit cycle L_0 ultimately (See Figure 5(b)).

Now, we will prove the case that the trajectory intersects with the impulse set Σ_M . We define that P point is the intersection of the image set Σ_N and the limit cycle L_0 . Take a point $P_1^- \in \Sigma_M$ which causes P_1^- runs to P after impulse effects, set $G(P_1^-) = P_1^+ \in \Sigma_M$ which makes P_2^- runs to P_1^+ after the impulse effects, then $y_P > y_{P_1^+}$, $y_{P_1^-} > y_{P_2^-}$. This process is continuing until there exists a $P_{m+k}^+ \in \Sigma_N$ satisfying $y_{P_{m+k}^+} < \tau$. As a result, we obtain a sequence $\{P_i^+\}_{i=1,2,\dots,m+k}$ of set Σ_N satisfying $G(P_{m+k}^+) = P_{m+k}^-$ and $y_{P_{m+k}^+} < y_{P_{m+k-1}^+}$. Due to the coincidence of P_{m+k}^+ and D , we can get $G(D) = P_{m+k}^-$ and $y_D < y_{P_{m+k-1}^+}$. In

the following part, we will prove the trajectory of system (2.3) initiating any point of set will go on for approaching the limit cycle L_0 ultimately.

From the vector field of System (2.5), we know the trajectory of System (2.5) initiating any point above P point of the image set Σ_N will be free from impulse effect and approach the limit cycle L_0 ultimately.

For any point is below P point, it must lie between P_{m+k}^+ and P_{i-1}^+ , where $i = 1, 2, \dots, m+k$ and $P_{m+k}^+ = D$. After i times' impulse effects, the trajectory initiating this point will arrive at some points of the image set Σ_N and must be above P , and then approach the limit cycle L_0 ultimately (See Figure 5(a)).

According above analysis, we know that the trajectory will tend to the limit cycle L_0 ultimately. The proof has been done.

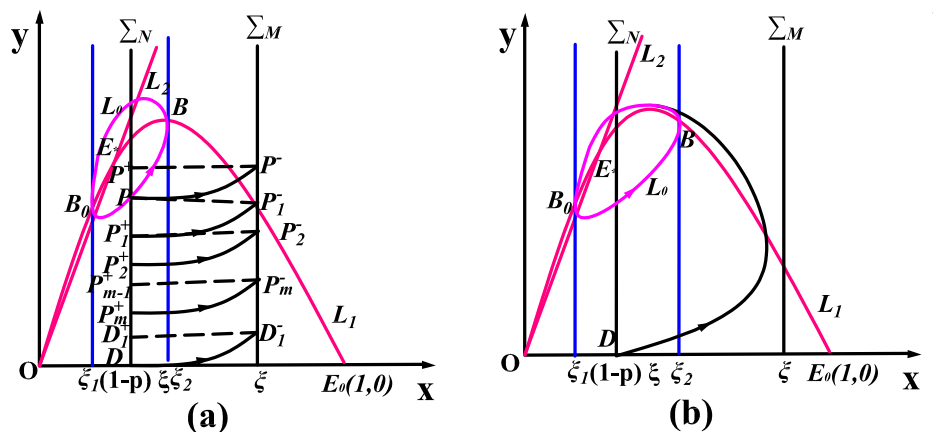


Figure 5. When $\xi > \max\{\xi_2, \xi_{min}\}$ and $\xi_1 < (1-p)\xi < \xi_2$. (a) The trajectory Γ_0 can hit the impulse set Σ_M . (b) The trajectory Γ_0 can not hit the impulse set Σ_M .

□

4. Simulations and optimization

4.1. Numerical simulations

To prove the feasibility of this conclusion, some simple examples are given in this section.

Let $\alpha_1 = 0.6$, $\alpha_2 = 0.8$, $\beta = 1.2$ and we shall get the internal equilibrium points of system (2.3) is $E_* = (0.53, 0.43)$, where E_* is a stable node. Let $p = 0.65$, $q = 0.15$, $\tau = 0.2$ and we shall get a unique order-1 periodic solution and it is asymptotically stable (see Figure 6). What's more, we can get the period of order-1 periodic solution is $T = 5.081$.

Let $\alpha_1 = 0.75$, $\alpha_2 = 0.15$, $\beta = 0.05$, then we can get the positive equilibrium point is $E_* =$

(0.294, 0.441), and it is a stable focus. When $\xi = 0.32$, $p = 0.4$, $q = 0.2$, $\tau = 0.1$, and the system (2.3) has an order-1 periodic solution and the solution is unique and asymptotically stable. What's more, we can get the period of order-1 periodic solution is $T = 3.9625$ (see Figure 7).

Let $\alpha_1 = 0.75$, $\alpha_2 = 2$, and $\beta = 0.05$, then we shall get the interval equilibrium point $E_* = (0.2, 0.4)$ is a unstable focus, and there exists an unique limit cycle.

(i) Let $\xi = 0.2$, $p = 0.4$, $q = 0.2$, $\tau = 0.1$ and the initial value is (0.15, 0.3), the system (2.3) possesses order-1 periodic solution (see Figure 8).

(ii) Let $\xi = 0.6$, $p = 0.3$, $q = 0.2$, $\tau = 0.15$ and the initial value is (0.1, 0.18), then the trajectory Γ_0 can not hit the impulse set Σ_M , therefore system (2.3) does not possess order-1 periodic solution and the trajectory Γ_0 tend to the limit cycle (see Figure 9).

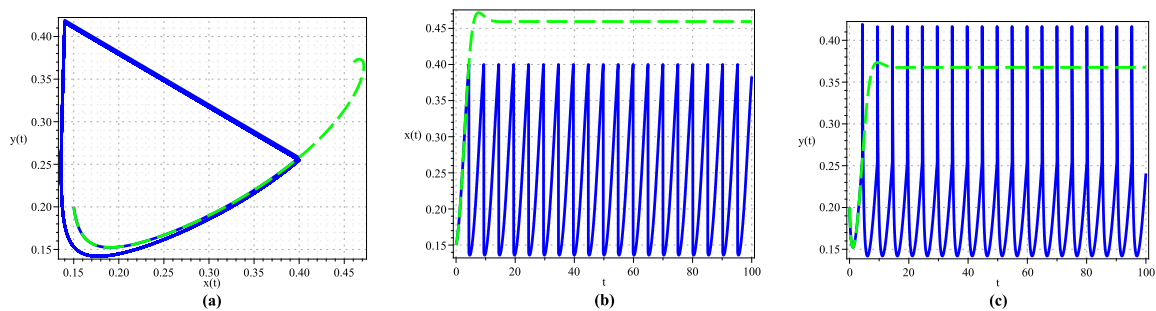


Figure 6. Numerical simulations when $0 < \xi < \min\{x_*, \xi_{min}\}$ and $(\alpha_1\alpha_2 + 2) < (\beta\alpha_2 + 1)(\alpha_1\alpha_2 + 1)^2$ hold and the initial value is (0.15, 0.2). (a) Phase portrait of $x(t)$ and $y(t)$ on $\xi = 0.4$. (b) Time series of $x(t)$. (c) Time series of $y(t)$. The solution of system (2.3) is presented in blue full line and the solution of free System (2.5) is represented in green dotted lines.

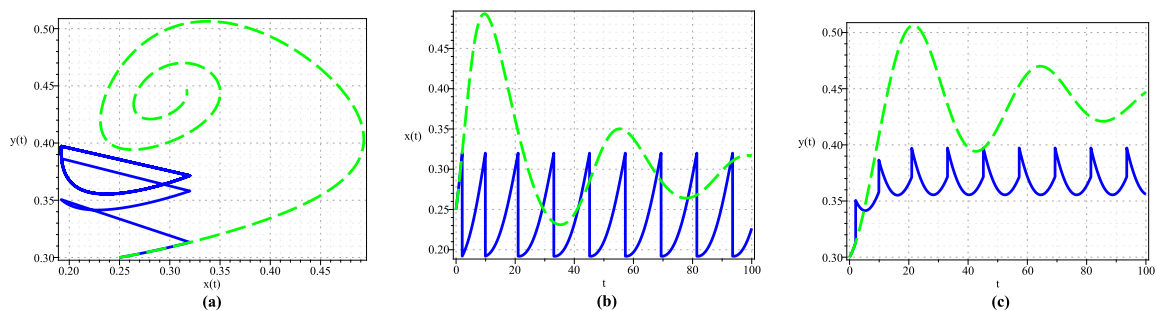


Figure 7. Numerical simulations when $\max\{x_*, \xi_{max}\} < \xi < 1$, $(\alpha_1\alpha_2 + 2) < (\beta\alpha_2 + 1)(\alpha_1\alpha_2 + 1)^2$ hold and the initial value is (0.25, 0.3). (a) Phase portrait of $x(t)$ and $y(t)$ on $\xi = 0.32$. (b) Time series of $x(t)$. (c) Time series of $y(t)$. The solution of system (2.3) is presented in blue full line and the solution of free System (2.5) is represented in green dotted lines.

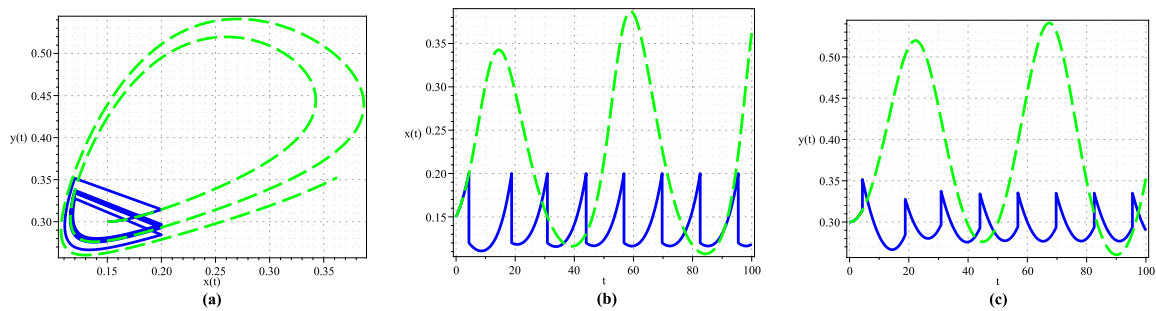


Figure 8. Numerical simulations E_* is an unstable focus and the trajectory Γ_0 can hit the impulse set Σ_M . (a) phase diagram. (b) Time series of $x(t)$. (c) Time series of $y(t)$. The solution of system (2.3) is presented in blue full line and the solution of free System (2.5) is represented in green dotted lines.

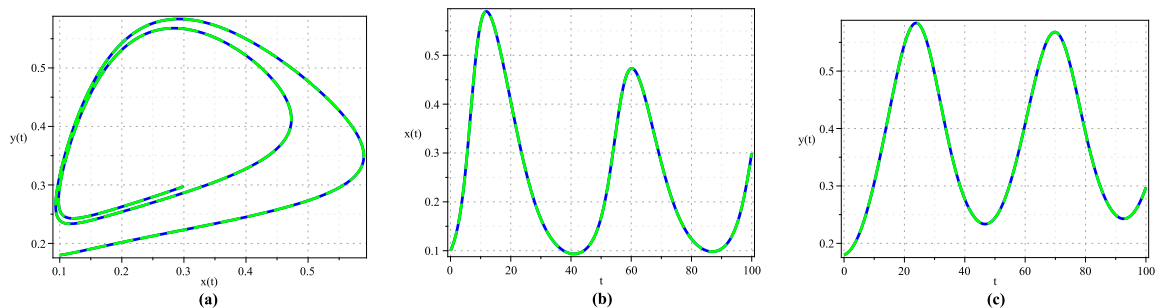


Figure 9. Numerical simulations E_* is an unstable focus and the trajectory Γ_0 can not hit the impulse set Σ_M . (a) phase diagram. (b) Time series of $x(t)$. (c) Time series of $y(t)$. The solution of system (2.3) is presented in blue full line and the solution of free System (2.5) is represented in green dotted lines.

4.2. Determination of optimal threshold ξ

The practical significance of the research of order-1 periodic solution is that it provides a possibility to determine the adding rate of beneficial insects and insect pest eradication rate, this makes the pulse control no longer the real-time monitor of agricultural production, but a cyclical. To maintain the balance of ecological agriculture, to further determine the optimal replenishment of beneficial insects rate and the rate of eliminating most pests, and to ensure the longest administer interval period, the lowest cost, we study the following optimization problem to find the optimal threshold ξ .

We define s_1 as the unit cost of supplementary natural enemies including the cost of processing agricultural environment, and denote s_2 as the unit cost of insecticide spraying. Our goal is to minimize costs this process. V_{cost} is defined as the total cost in under the control of threshold ξ one period of model (2.3), and it is a function about the rate τ of natural enemies replenishment and the rate p of killed pest, that means $V_{cost}(\xi) = s_1\tau(\xi) + s_2p(\xi)$. Therefore, we formulated the optimization model as

$$\min \frac{V_{cost}(\xi)}{T(\xi)},$$

s.t. $\xi_{min} < \xi < \xi_{max}$.

Table 1. Value of parameters of Figure 10.

ξ	p	q	τ	T	$\frac{V_{cost}}{T}$
0.15	0.094	0.038	0.886	18.723	105.0
0.20	0.186	0.075	0.775	19.345	99.0
0.25	0.281	0.113	0.663	19.735	96.0
0.33	0.431	0.173	0.483	19.967	91.4
0.35	0.469	0.188	0.438	19.867	91.7
0.40	0.563	0.225	0.325	19.500	92.0
0.45	0.656	0.263	0.213	18.720	92.8

We solve the optimization problem to obtain the optimal threshold ξ^o , and we get the optimal replenishment rate of natural enemy $\tau^o = \tau(\xi^o)$, the optimal chemical control strength $p^o = p(\xi^o)$ and the optimal impulse period $T^o = T(\tau^o, p^o)$.

Let $\alpha_1 = 0.75$, $\alpha_2 = 1.5$, $\beta = 0.05$, $\xi_{min} = 0.1$, $\xi_{max} = 0.5$, $\tau_{min} = 0.1$, $\tau_{max} = 1$, $p_{max} = 0.75$, $q_{max} = 0.3$, taking these parameters into system (2.3) and system (2.4), we shall get the following equations

$$\begin{cases} x'(t) = x(t) - x^2(t) - \frac{x(t)y(t)}{0.75y(t) + x(t)}, \\ y'(t) = 0.075y(t) - \frac{0.05y^2(t)}{x(t)}. \end{cases} \quad (4.1)$$

$$\begin{cases} p(x) = 0.9375(x - 0.1), \\ \tau(x) = 0.8 - x, \\ q(x) = 0.25(x - 0.1). \end{cases} \quad (4.2)$$

Bringing the values of parameter ξ into system (4.2) can calculate the values of parameters p , q , τ . The period T can be obtained by numerical simulation. Therefore, the relationship between impulse period T and the threshold ξ is obtained in Figure 10(a) (the relevant dates in figure are shown in Table 1). Set $s_1 = 2000$, $s_2 = 2000$, by calculation we can get the value of V_{cost}/T . The relationship between the cost per unit time V_{cost}/T and the threshold ξ is shown in Figure 10(b) (the relevant dates in figure are shown in Table 1). As is shown in Figure 10, we can obtain the optimal threshold $\xi^o = 0.33$, the optimum yield of releases of the natural enemies is $\tau^o = 0.483$, the optimal killing rate of natural enemies is $p^o = 0.431$, and the optimal impulse period is $T^o = 19.967$. Therefore, the control measures are adopted when the density of pests ξ reaches 0.33. Furthermore, it should be noted that the optimum pest control level ξ^o is dependent on the ratio of $\omega = \frac{s_2}{s_1}$, as illustrated in Figure 11 (the relevant dates in figure are shown in Table 2).

5. Conclusion

This paper puts forward a kind of ratio dependence and double pulse control feeding system, which is more practical than continuous single pulse control strategy. At the same time, we obtain the following conclusions:

(1) When $\alpha_1 \cdot \alpha_2 + 1 > \alpha_2$, $(\alpha_1\alpha_2 + 2)\alpha_2 < (\beta\alpha_2 + 1)(\alpha_1\alpha_2 + 1)^2$ and $(1 - q) |\Theta(f_0, g_0)| < |\Theta(f_1, g_1)|$,

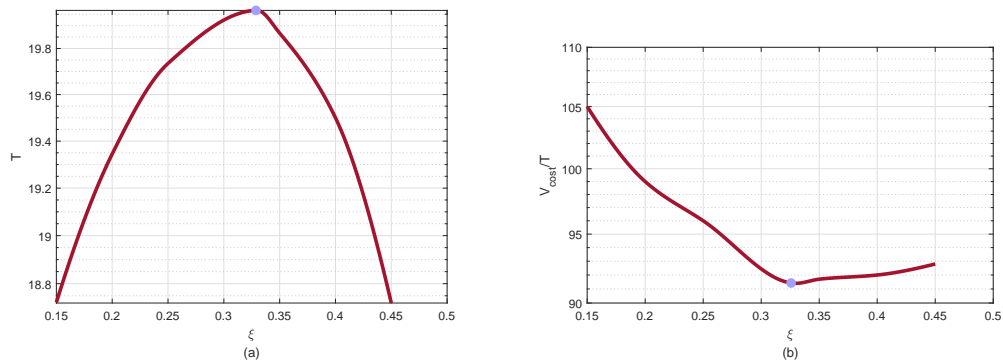


Figure 10. (a) The period T of the order-1 periodic solution varies with the threshold ξ . (b) The cost per unit time V_{cost}/T on the threshold ξ .

Table 2. Value of parameters of Figure 11.

ξ	$\frac{V_{cost}}{T} (\frac{s_2}{s_1} = \frac{1}{2})$	$\frac{V_{cost}}{T} (\frac{s_2}{s_1} = 1)$	$\frac{V_{cost}}{T} (\frac{s_2}{s_1} = 2)$	$\frac{V_{cost}}{T} (\frac{s_2}{s_1} = 5)$
0.15	99.7	105.0	57.0	72.4
0.2	89.7	99.0	59.3	88.1
0.25	81.4	96.0	62.1	104.8
0.33	70.0	91.4	67.4	132.1
0.35	67.7	91.7	69.3	140.0
0.4	62.2	92.0	74.0	161.0
0.45	57.8	92.8	81.5	187.0

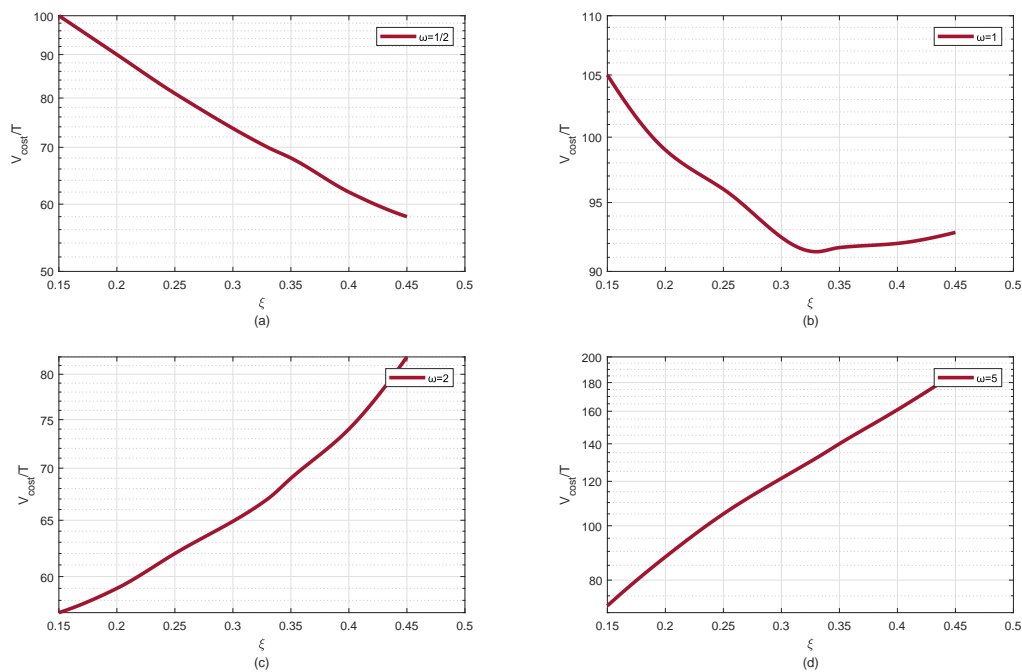


Figure 11. The change in the cost per unit time $\frac{V_{cost}}{T}$ on the pest control level ξ for $\omega = 1/2, 1, 2, 5$.

we can obtain the existence, uniqueness and orbital asymptotical stability of the order-1 periodic solution for system (2.3).

(2) When $\max\{x_*, \xi_{min}\} < \xi < 1$, $\alpha_1 \cdot \alpha_2 + 1 > \alpha_2$ and $(\alpha_1\alpha_2 + 2)\alpha_2 < (\beta\alpha_2 + 1)(\alpha_1\alpha_2 + 1)^2$, the system (2.3) has order-1 periodic solution.

(3) When the equilibrium $E_*(x_*, y_*)$ is an unstable focus and conditions $\alpha_1\alpha_2 + 1 > \alpha_2$, $(\alpha_1\alpha_2 + 2)\alpha_2 > (\beta\alpha_2 + 1)(\alpha_1\alpha_2 + 1)^2$, $\xi > \max\{\xi_2, \xi_{min}\}$, $\xi_1 < (1 - p)\xi$ and $y_{C^+} > y_C$ hold, the trajectory of system (2.3) will approach to the limit cycle L_0 in the end.

(4) We formulate the optimization mode and obtain optimal threshold, optimal replenishment rate of natural enemies and optimal chemical control strength. In the example in Section 4.2, we get the optimal threshold, the optimum yield of releases of the natural enemies, the optimal killing rate of natural enemies and the optimal impulse period are 0.33, 0.483, 0.431 and 19.967, respectively. In the end, we can minimize the cost of controlling pests.

Our results show that under certain conditions, pest population can be controlled within the threshold, while pests and natural enemies change periodically. Further, we propose the optimal control strategy of pests, which provides a theoretical basis for production labor.

Compared with the literature [48], this paper adds impulse feedback control to the model, so this paper is a further study of [48]. Literature [46] and [51] proposed Leslie-Gower prey-predator models with different impulse feedback controls and discussed the existence, uniqueness and stability of order-1 periodic solution. Based on this, this paper further studies the optimal control strategy of pest management.

In real life, the optimization of plague control is also a hot topic for some scholars [53]. We will further improve the optimization control strategy to make our research work more realistic and meaningful.

Acknowledgements

The paper was supported by the National Natural Science Foundation of China (No.11371230), Shandong Provincial Natural Science Foundation, China (No. S2015SF002), SDUST Innovation Fund for Graduate Students(SDKDYC190351), SDUST Research Fund (2014TDJH102), and Joint Innovative Center for Safe and Effective Mining Technology and Equipment of Coal Resources, Shandong Province of China.

Conflict of interest

The authors declare that there is no conflict of interests regarding the publication of this paper.

References

1. H. Guo and X. Song, An impulsive predator-prey system with modified Leslie-Gower and Holling type II schemes, *Chaos Solitons Fract.*, **36** (2008), 1320–1331.
2. R. Kooij, J. Arus and A. Embid, Limit cycles in the Holling-Tanner model, *Publicacions Matematiques*, **41** (1997), 149–167.

3. F. Wang, H. Cheng and Q. Li, Dynamic analysis of wild and sterile mosquito release model with Poincaré map, *Math. Biosci. Eng.*, **16** (2019), 7688–7706.
4. F. Zhu, X. Meng and T. Zhang, Optimal harvesting of a competitive n-species stochastic model with delayed diffusions, *Math. Biosci. Eng.*, **16** (2019), 1554–1574.
5. Y. Li, Y. Li, Y. Liu, et al., Stability analysis and control optimization of a prey-predator model with linear feedback control, *Discrete Dyn. Nature Soc.*, **2018** (2018), 4945728.
6. C. Li and S. Tang, Analyzing a generalized pest-natural enemy model with nonlinear impulsive control, *Open Math.*, **16** (2018), 1390–1411.
7. J. Gu, Y. Zhang and H. Dong, Dynamic behaviors of interaction solutions of (3+1)-dimensional shallow water wave equation, *Comput. Math. Appl.*, **76** (2018), 1408–1419.
8. Z. Shi, J. Wang, Q. Li, et al., Control optimization and homoclinic bifurcation of a prey-predator model with ratio-dependent, *Adv. Differ. Equ.*, **2019** (2019), 2.
9. Y. Tian, S. Tang and R. A. Cheke, Nonlinear state-dependent feedback control of a pest-natural enemy system, *Nonlinear Dyn.*, **94** (2018), 2243–2263.
10. Y. Li, H. Cheng, J. Wang, et al, Dynamic analysis of unilateral diffusion Gompertz model with impulsive control strategy, *Adv. Differ. Equ.*, **2018** (2018), 32.
11. T. Zhang, Y. Song, T. Zhang, et al, A stage-structured predator-prey SI model with disease in the prey and impulsive effects, *Math. Model. Anal.*, **18** (2013), 505–528.
12. Z. Shi, Y. Li and H. Cheng, Dynamic analysis of a pest management smith model with impulsive state feedback control and continuous delay, *Mathematics*, **7** (2019), 591.
13. Z. Jiang, X. Bi, T. Zhang, et al., Global hopf bifurcation of a delayed phytoplankton-zooplankton system considering toxin producing effect and delay dependent coefficient, *Math. Biosci. Eng.*, **16** (2019), 3807–3829.
14. Y. Li, H. Cheng and Y. Wang, A *Lycaon pictus* impulsive state feedback control model with Allee effect and continuous time delay, *Adv. Differ. Equ.*, **2018** (2018), 367.
15. K. Liu, T. Zhang and L. Chen, State-dependent pulse vaccination and therapeutic strategy in an SI epidemic model with nonlinear incidence rate, *Comput. Math. Method. M.*, **2019** (2019), article ID 3859815.
16. F. Wang, B. Chen, Y. Sun, et al., Finite time control of switched stochastic nonlinear systems, *Fuzzy Set. Syst.*, **35** (2019), 140–152.
17. S. Tang, X. Tan, J. Yang, et al., Periodic solution bifurcation and spiking dynamics of impacting predator-prey dynamical model, *Int. J. Bifurcat. Chaos*, **28** (2018), 1850147.
18. G. Pang and L. Chen, Periodic solution of the system with impulsive state feedback control, *Nonlinear Dyn.*, **78** (2014), 743–753.
19. Z. Zhao, L. Pang and X. Song, Optimal control of phytoplankton fish model with the impulsive feedback control, *Nonlinear Dyn.*, **88** (2017), 2003–2011.
20. Y. Gong and J. Huang, Bogdanov-takens bifurcation in a Leslie-Gower predator-prey model with prey harvesting, *Acta Math. Appl. Sin-E*, **30** (2014), 239–244.

21. T. Zhang, X. Meng and Y. Song, The dynamics of a high-dimensional delayed pest management model with impulsive pesticide input and harvesting prey at different fixed moments, *Nonlinear Dyn.*, **64** (2011), 1–12.
22. J. Jiao, L. Chen, J. Nieto, et al., Permanence and global attractivity of stage-structured predator-prey model with continuous harvesting on predator and impulsive stocking on prey, *Appl. Math. Mech.*, **195** (2008), 316–325.
23. Y. Pei, C. Li and L. Chen, Continuous and impulsive harvesting strategies in a stage-structured predator-prey model with time delay, *Math. Comput. Simulat.*, **79** (2009), 2994–3008.
24. J. Jiao, S. Cai and L. Li, Dynamics of a periodic switched predator-prey system with impulsive harvesting and hibernation of prey population, *J. Franklin I.*, **353** (2016), 3818–3834.
25. K. Sun, T. Zhang and Y. Tian, Dynamics analysis and control optimization of a pest management predator-prey model with an integrated control strategy, *Appl. Math. Comput.*, **292** (2017), 253–271.
26. S. Tang and L. Chen, Global attractivity in a food-limited population model with impulsive effects, *J. Math. Anal. Appl.*, **292** (2004), 211–221.
27. Z. Shi, H. Cheng, Y. Liu, et al., A *Cydia Pomonella* integrated management predator-prey model with smith growth and linear feedback control, *IEEE ACCESS*, **7** (2019), 126066–126076.
28. P. H. Leslie, Some further notes on the use of matrices in population mathematics, *Biometrika*, **35** (1948), 213–245.
29. F. Liu, Q. Xue and K. Yabuta, Boundedness and continuity of maximal singular integrals and maximal functions on triebel-lizorkin spaces, *Sci. China-Math.*, Mathematics, Doi: 10.1007/s11425-017-9416-5.
30. J. Wang, H. Cheng, X. Meng, et al., Geometrical analysis and control optimization of a predator-prey model with multi state-dependent impulse, *Adv. Differ. Equ.*, **2017** (2017), 252.
31. W. Lv and W. Fang, Adaptive tracking control for a class of uncertain nonlinear systems with infinite number of actuator failures using neural networks, *Adv. Differ. Equ.*, **2017** (2017), 374.
32. Z. Zhao, Z. Li and L. Chen, Existence and global stability of periodic solution for impulsive predator-prey model with diffusion and distributed delay, *J. Appl. Math. Comput.*, **33** (2010), 389–410.
33. P. H. Leslie and J. C. Gower, The properties of a stochastic model for the predator-prey type of interaction between two species, *Biometrika*, **47** (1960), 219–234.
34. H. Liu and H. Cheng, Dynamic analysis of a prey-predator model with state-dependent control strategy and square root response function, *Adv. Differ. Equ.*, **2018** (2018), 63.
35. J. Wang, H. Cheng, H. Liu, et al., Periodic solution and control optimization of a prey-predator model with two types of harvesting, *Adv. Differ. Equ.*, **2018** (2018), 41.
36. T. Liu and H. Dong, The Prolongation Structure of the Modified Nonlinear Schrödinger Equation and Its Initial-Boundary Value Problem on the Half Line via the Riemann-Hilbert Approach *Mathematics*, **7** (2019), 170.
37. Q. Wang, Y. Zhang, Z. Wang, et al., Periodicity and attractivity of a ratio-dependent Leslie system with impulses, *J. Math. Anal. Appl.*, **376** (2011), 212–220.

38. S. Tang, B. Tang, A. Wang, et al., Holling II predator-prey impulsive semi-dynamic model with complex Poincaré map, *Nonlinear Dyn.*, **81** (2015), 1575–1596.
39. T. Zhang, X. Liu, X. Meng, et al., Spatio-temporal dynamics near the steady state of a planktonic system, *Comput. Math. Appl.*, **75** (2018), 4490–4504.
40. M. Han, L. Zhang, Y. Wang, et al., The effects of the singular lines on the traveling wave solutions of modified dispersive water wave equations, *Nonlinear Anal-Real.*, **47** (2019), 236–250.
41. F. Liu, Z. Fu and S. T. Jhang, Boundedness and continuity of marcinkiewicz integrals associated to homogeneous mappings on Triebel-Lizorkin spaces, *Front. Math. China*, **14** (2019), 95–122.
42. F. Liu, Rough maximal functions supported by subvarieties on Triebel-Lizorkin spaces *Revista de la Real Academia de Ciencias Exactas, Físicas y Naturales. Serie A. Matemáticas*, **112** (2018), 593–614.
43. X. Meng, F. Li and S. Gao, Global analysis and numerical simulations of a novel stochastic ecoepidemiological model with time delay, *Appl. Math. Comput.*, **339** (2018), 701–726.
44. R. P. Gupta and M. Banerjee, Bifurcation analysis and control of Leslie-Gower predator-prey model with Michaelis-Menten type prey-harvesting, *Differ. Equ. Dyn. Syst.*, **20** (2012), 339–366.
45. Z. Zhao, L. Yang and L. Chen, Impulsive perturbations of a predator-prey system with modified Leslie-Gower and Holling type II schemes *J. Appl. Math. Comput.*, **35** (2011), 119–134.
46. C. Wei and L. Chen, A Leslie-Gower pest management model with impulsive state feedback control, *J. Biomath.*, **27** (2012), 621–628.
47. J. D. Flores and E. González-Olivares, A modified Leslie-Gower predator-prey model with ratio-dependent functional response and alternative food for the predator, *Math. Methods Appl. Sci.*, **40** (2017), 2313–2328.
48. Z. Liang and H. Pan, Qualitative analysis of a ratio-dependent Holling-Tanner model, *Math. Anal. Appl.*, **334** (2007), 954–964.
49. K. Sun, T. Zhang and Y. Tian, Theoretical study and control optimization of an integrated pest management predator-prey model with power growth rate, *Math. Biosci.*, **279** (2012), 13–26.
50. C. Wei, J. Liu and L. Chen, Homoclinic bifurcation of a ratio-dependent predator-prey system with impulsive harvesting, *Nonlinear Dyn.*, (2017), 1–12.
51. Z. Liang, X. Zeng, G. Pang, et al., Periodic solution of a Leslie predator-prey system with ratio-dependent and state impulsive feedback control *Nonlinear Dyn.*, (2017), 1–15.
52. Y. Tian, K. Sun and L. Chen, Geometric approach to the stability analysis of the periodic solution in a semi-continuous dynamic system, *Int. J. Biomath.*, **7** (2014), 1450018.
53. C. J. Edholm, B. Tenhumberg, C. Guiver, et al., Management of invasive insect species using optimal control theory, *Ecol. Model.*, **381** (2018), 36–45.



AIMS Press

©2019 the Author(s), licensee AIMS Press. This is an open access article distributed under the terms of the Creative Commons Attribution License (<http://creativecommons.org/licenses/by/4.0>)